Mon. Not. R. astr. Soc. (1985) **212**, 837–850

Shapes of planetary nebulae

F. D. Kahn and Kym A. West *Department of Astronomy, The University, Manchester M13 9PL*

Accepted 1984 September 26. Received 1984 September 21; in original form 1984 July 5

Summary. The formation of planetary nebulae can be discussed in terms of an interacting stellar winds model, in which the slow wind from the progenitor star is later overtaken by the fast wind from the central star. As a result of the interaction the inner region of the slow wind is compressed into a dense shell. We investigate the consequences for the model of a red-giant wind in which the mass-loss rate is enhanced towards the equator. The resulting shell is elongated in the direction of the poles. Our treatment is simplified, in that we neglect the finite temperature of the compressed shell. Consequently, the cusps which we sometimes find at the equator are, in reality, regions of high density.

1 Introduction

The existence of slow ($\sim 10\,\mathrm{km\,s^{-1}}$) winds from red-giant stars and of fast ($\sim 1000\,\mathrm{km\,s^{-1}}$) winds from several central stars of planetary nebulae (PNe) is well established. The interacting stellar winds model (Kwok 1982; Kahn 1982) is based on the assumption that the gas ejected by the red-giant wind, the red-giant envelope, still surrounds the central star when the fast wind switches on. The fast wind interacts with this medium in a manner similar to that of the winds of OB stars (Dyson & de Vries 1972). Since, by definition, there is material cooler than the stellar wind around the central star, the fast wind will sweep it into a shell whether it has been ejected by a slow wind, is an ejected shell, or is material ejected by a transient superwind (Renzini 1982).

Having established the importance of the fast wind in PNe, we next look to see how we can reproduce some of their many different shapes. As the fast wind shocks close to the star, any asymmetries in its distribution will not be apparent in the shape of the PN. Kahn (1982) has discussed how an initially spherical shell may break up due to instabilities. In this paper, we investigate the effects of a red-giant mass-loss rate which depends on the polar angle, θ, in such a way as to increase from the pole to the equator, about which it is symmetrical.

2 The model

2.1 THE EXPANDING SHELL

In our model, the red-giant mass-loss rate per steradian is

$$\Phi(\theta) = \frac{\dot{M}(1 + \epsilon \sin^n \theta)}{\int_0^{4\pi} (1 + \epsilon \sin^n \theta)\, d\omega}, \tag{1}$$

where n is an integer. The speed of the wind, V, is about $10\,\mathrm{km\,s^{-1}}$ and is independent of θ and time. At time $t = 0$, we assume that the change from the slow wind to the fast wind occurs instantaneously. The fast wind is hypersonic and the standard two-shock pattern may be assumed to exist (Dyson & de Vries 1972). The temperature of the shocked wind is of order $10^7\,\mathrm{K}$, so radiation losses may be assumed negligible. The important parameter defining the properties of the fast wind is the rate of injection of thermal energy into the shocked wind, L_w, which determines the rate of expansion of the shell, U. However, we find it more convenient to specify U and determine L_w. The shell of matter swept up by the outward-moving shock is identified with the PN (or with the innermost shell of the PN if more than one exists), so U should be in the range 20–$50\,\mathrm{km\,s^{-1}}$. As this is much lower than the sound speed in the hot wind bubble, it is a good approximation to assume that the pressure inside the bubble is uniform.

The flow problem admits a similarity solution in which the radius of the shell, r, is proportional to time, so we can write

$$r(\theta, t) = UtF(\theta), \qquad F(0) = 1, \tag{2}$$

where $F(\theta)$ defines the shape of the shell, and is determined by $\Phi(\theta)$ and U. The angle between the radial vector, $\hat{\mathbf{r}}$, and the tangential vector, $\hat{\mathbf{t}}$, at a point on the shell is denoted by ϕ, and is related to the shell radius by

$$\tan\phi = \frac{r\,d\theta}{dr} = \frac{F}{F'}. \tag{3}$$

2.2 CONSERVED QUANTITIES

To derive a solution, we require a closed system of equations comprising conservation equations and the equation of motion.

2.2.1 Conservation of mass

The mass of the shell grows linearly with time, so we define the mass that lies within angle θ of the poles as

$$M(\theta, t) = \mathcal{M}(\theta)\, t. \tag{4}$$

The rate of inflow of mass into the cone of semi-angle θ is

$$\frac{dM}{dt}(\theta, t) = \int \frac{\Phi}{V}(UF - V)\, 2\pi \sin\theta\, d\theta. \tag{5}$$

Here d/dt is the convective derivative; on differentiation we find that

$$(1+\Theta')\mathscr{M}' + \Theta\mathscr{M}'' = 2\pi \sin\theta \frac{\Phi}{V}(UF - V), \tag{6}$$

where we have written $\dot{\theta}$ as $\Theta(\theta)/t$.

2.2.2 *Pseudo-angular momentum of an individual particle*

Before discussing the dynamics of the shell gas, it is useful to consider first a single particle. The particle is constrained to move on the surface of a shell expanding according to equation (2). The motion of the particle can be separated into a radial component, $\dot{r} = UF(\theta) + UF'(\theta)\Theta(\theta)$, and a transverse component, $r\dot{\theta} = UF(\theta)\Theta(\theta)$. The kinetic energy per unit mass of the particle is then

$$T = \tfrac{1}{2}(\dot{r}^2 + r^2\dot{\theta}^2). \tag{7}$$

There is no potential energy term, so Lagrange's equation is

$$\frac{d}{dt}\left(\frac{\partial T}{\partial \dot{\theta}}\right) - \frac{\partial T}{\partial \theta} = 0. \tag{8}$$

Using our definitions, this can be rewritten as

$$\frac{d}{dt}\left\{(F^2 + F'^2)^{1/2}\Theta t\right\} = 0, \tag{9}$$

which implies that,

$$j = (F^2 + F'^2)^{1/2}\Theta t \tag{10}$$

is a conserved quantity. The quantity $U^2 j$ has the dimensions of angular momentum per unit mass, so we call j pseudo-angular momentum per unit mass.

2.2.3 *Pseudo-angular momentum of the shell gas*

In considering the motion of the gas along the shell, we wish to make use of the conservation of pseudo-angular momentum, but there is an additional contribution to the equation of motion from the pressure gradient resolved along the shell. However, we shall show that this may be neglected provided that the shell is thin. In order to do so, we first estimate the pressure at a typical point in the shell. We recall that the pressure in the shocked wind bubble, P_0, is uniform but that the ram pressure of the swept-up material, P', depends on θ. The difference between P' and P_0 produces an acceleration of the shell gas along the direction of the normal to the shell. Accordingly,

$$P' - P_0 \sim \sigma r\Theta^2/t^2 = \sigma UF\Theta^2/t, \tag{11}$$

where σ is mass per unit area. Thus, the pressure at a typical point in the shell is

$$\frac{P' + P_0}{2} \sim \frac{\sigma UF\Theta^2}{2t} + P_0. \tag{12}$$

The average pressure gradient resolved along the shell is approximately

$$\frac{\sigma UF\Theta^2}{2t(r\pi/2)} \sim \frac{\sigma\Theta^2}{3t^2}. \tag{13}$$

This produces a contribution to the acceleration of

$$\frac{\sigma\Theta^2}{3\rho t^2} \sim \frac{\Theta^2 \delta r}{3t^2}, \tag{14}$$

where ρ is the density of the shell and δr is the thickness of the shell. The transverse acceleration of the gas is

$$r\ddot{\theta} + 2\dot{r}\dot{\theta} = \frac{U\Theta}{t}[F(1+\Theta') + 2F'\Theta] \sim \frac{U\Theta F}{t} = \frac{r\Theta}{t^2}. \tag{15}$$

The tangential acceleration is of the same order as the above and, therefore, much larger than the term in equation (14), provided that the shell is thin. [The term $F(1+\Theta') + 2F'\Theta$ is actually less than F for large θ because both Θ' and $F'\Theta$ are negative. However, $|F'\Theta|$ has its maximum value for $\Theta' \sim 0$, and we find from our solutions that the value of Θ rarely exceeds 0.2. So, although F' can approach -1, the product, $|F'\Theta|$, is generally quite small. The value of Θ' can approach -1, when $F'\Theta$ is close to zero, but this requires very large values of both ϵ and n, and only applies to a small range of θ near the equator.]

For the shell gas the quantity conserved is the mass-weighted pseudo-angular momentum per unit mass. So we define $J(\theta, t)$ as the integrated product of mass per steradian and j over the cone of semi-angle θ, that is

$$J(\theta, t) = \int \mathscr{M}' t j \, d\theta$$

$$= \mathscr{J}(\theta)\, t^2 \tag{16}$$

where

$$\mathscr{J}(\theta) = \int \mathscr{M}' (F^2 + F'^2)^{1/2} \Theta \, d\theta. \tag{17}$$

In order to derive the conservation equation, we need to know the pseudo-angular momentum of the swept-up gas, j_0. We consider a reference frame in which the shock is at rest. The gas entering the shock has velocity $(UF - V)$ directed radially inwards. We assume that the shock is well-cooled so that the velocity component normal to the shock is annihilated. The tangential component is unaffected and can be written in terms of radial and transverse components. In the rest frame of the star, these are

$$\dot{r} = UF - (UF - V)\cos^2\phi \tag{18}$$

and

$$r\dot{\theta} = -(UF - V)\sin\phi\cos\phi. \tag{19}$$

With the aid of equation (10), we note that the motion of the incoming gas can be decomposed into a radial component, UF, and a component, Uj_0/t, along the meridional curve. Comparison with equation (19) then leads to the following expression for j_0:

$$j_0 = t\frac{(V - UF)}{U}\cos\phi. \tag{20}$$

The rate of change of $J(\theta, t)$ with time can now be derived, and is given by

$$\frac{dJ}{dt}(\theta, t) = \int \frac{\Phi}{V}(UF - V)\, 2\pi \sin\theta \left(\frac{V}{U} - F\right) t \cos\phi \, d\theta. \tag{21}$$

If we then substitute from equation (17), differentiate both sides with respect to θ and divide through by t, we obtain

$$(2+\Theta')\,\mathscr{J}' + \Theta\mathscr{J}'' = \frac{-2\pi\sin\theta F'}{UV(F^2+F'^2)^{1/2}}\,\Phi(UF-V)^2. \tag{22}$$

By rearranging equation (17), we derive

$$\frac{d\mathscr{J}}{d\mathscr{M}} = \frac{\mathscr{J}'}{\mathscr{M}'} = (F^2+F'^2)^{1/2}\Theta. \tag{23}$$

2.2.4 *Pressure*

A further equation can be derived by considering the balance of pressures. The force per unit area required to keep the gas moving around the curved surface of the shell must equal the difference between the ram pressure and the pressure of the hot shocked wind gas. It can be written as the product of the mass per unit area of the shell, σ, and the acceleration resolved along the normal. σ is derived by considering the shell segment between the cones of semi-angles θ and $\theta + d\theta$. The mass of this segment is

$$M(\theta+d\theta,t) - M(\theta,t) = \mathscr{M}'(\theta)\,t\,d\theta \tag{24}$$

and the area of the surface is

$$\delta A = 2\pi r^2 \sin\theta\, d\theta \operatorname{cosec}\phi, \tag{25}$$

thus

$$\sigma = \frac{\mathscr{M}'(\theta)}{2\pi\sin\theta\, U^2F(F^2+F'^2)^{1/2}}\,\frac{1}{t}. \tag{26}$$

The acceleration directed outwards along the normal to the shell is

$$a = [(\ddot{r} - r\dot{\theta}^2)\sin\phi - (r\ddot{\theta} + 2\dot{r}\dot{\theta})\cos\phi]$$

$$= \frac{U\Theta^2}{(F^2+F'^2)^{1/2}t}\,[F^2 + 2F'^2 - FF'']. \tag{27}$$

The pressure of the hot wind bubble is derived by equating the energy in the bubble with the input from the stellar wind minus the loss due to the expansion of the bubble, and is

$$P_0 = \frac{2}{9}\frac{L_w}{\mathscr{V}}\frac{1}{t^2}, \tag{28}$$

where

$$\mathscr{V} = \frac{\mathscr{V}}{t^3} = \frac{2}{3}\pi U^3\int_0^{\pi} F^3\sin\theta\, d\theta, \tag{29}$$

and $\mathscr{V}$ is the volume of the bubble. The ram pressure of the newly swept-up gas is

$$P' = \frac{\Phi(UF-V)^2\sin^2\phi}{VU^2F^2t^2}$$

$$= \frac{\Phi(UF-V)^2}{U^2V(F^2+F'^2)}\,\frac{1}{t^2}. \tag{30}$$

Combining equations (26)–(28) and (30), we get

$$\frac{2}{9}\frac{L_w}{\nu}+\frac{\mathcal{M}'(F^2+2F'^2-FF'')}{2\pi UF(F^2+F'^2)\sin\theta}\Theta^2=\frac{\Phi(UF-V)^2}{U^2V(F^2+F'^2)}. \tag{31}$$

2.2.5 The solution

Equations (6), (22) and (31) are rewritten in terms of

$$\lambda=\frac{U}{V},\qquad q(\theta)=\frac{\Phi(\theta)}{\Phi(0)}=1+\epsilon\sin^n\theta,\qquad \mu(\theta)=\frac{\mathcal{M}'(\theta)}{\Phi(0)},$$

$$\gamma(\theta)=\frac{\mathcal{J}'(\theta)}{\Phi(0)},\qquad \tau=\frac{\nu}{U^3}\qquad \text{and}\ \Lambda_w=\frac{L_w}{\Phi(0)V^2},$$

and then rearranged to produce the following coupled differential equations

$$\frac{d}{d\theta}(\Theta\mu)=2\pi\sin\theta q(\lambda F-1)-\mu, \tag{32}$$

$$\frac{d}{d\theta}(\Theta\gamma)=\frac{-2\pi\sin\theta F'}{\lambda(F^2+F'^2)^{1/2}}q(\lambda F-1)^2-2\gamma, \tag{33}$$

$$\frac{d}{d\theta}\left(\tan^{-1}\frac{F}{F'}\right)=-1+\frac{2\pi F\sin\theta}{\mu\Theta^2}\left[\frac{q(\lambda F-1)^2}{\lambda(F^2+F'^2)}-\frac{2\Lambda_w}{9\tau\lambda^2}\right]. \tag{34}$$

The set is closed with the equation

$$\frac{d}{d\theta}F=F'. \tag{35}$$

A further equation, derived from equation (23),

$$\mu\Theta=\gamma/(F^2+F'^2)^{1/2}, \tag{36}$$

is used to disentangle the values of the variables after obtaining the solution of the differential equations. As the equations stand, it is necessary to know the value of L_w, which we said we would derive from the input value of U. By equating the terms of zeroth order in equation (34), one finds that

$$\tau=\frac{2\Lambda_w}{9\lambda(\lambda-1)^2}, \tag{37}$$

so that equation (34) can be rewritten as

$$\frac{d}{d\theta}\left(\tan^{-1}\frac{F}{F'}\right)=-1+\frac{2\pi F\sin\theta}{\mu\Theta^2}\left[\frac{q(\lambda F-1)^2}{\lambda(F^2+F'^2)}-\frac{(\lambda-1)^2}{\lambda}\right]. \tag{38}$$

3 Analytical approximations

It is possible to derive an analytical approximation to the above set of differential equations both near the pole, $\theta=0$ and near the equator, $\theta=\pi/2$. The former is required to start the

solution on the computer, while the latter provides information on the form of the solution near the equator (e.g. whether a cusp should be present there).

3.1 NEAR THE POLE

For small values of θ, $\sin\theta \sim \theta$, so we can approximate

$$q(\theta) \sim 1 + \epsilon\theta^n. \tag{39}$$

The mass within angle θ of the pole is proportional to the solid angle, and so varies like θ^2. As it is also proportional to $\int \mu\, d\theta$, we can approximate

$$\mu(\theta) \sim \mu_1 \theta. \tag{40}$$

The other variables can also be expanded in terms of θ. We write the expression for F as

$$F(\theta) \sim 1 + \frac{F_m}{m!}\theta^m + \ldots, \tag{41}$$

and for γ as

$$\gamma(\theta) \sim \frac{\gamma_m}{m!}\theta^m + \ldots. \tag{42}$$

Then, using these expressions in equation (36), we find that we can approximate Θ as

$$\Theta(\theta) \sim \frac{\Theta_{m-1}}{(m-1)!}\theta^{m-1}, \tag{43}$$

and we derive the relation

$$\gamma_m = m\Theta_{m-1}\mu_1. \tag{44}$$

We have already equated the terms of lowest order (zero) in equation (38). In equating the terms of the next order, we find that there are three possibilities:

(1) $n = m < 2(m-1)$,

(2) $n = 2(m-1) < m$,

(3) $m = 2(m-1) \leqslant n$.

Condition (1) can be satisfied for $n > 3$, condition (2) cannot be satisfied for reasonable values of n and m, and condition (3) is satisfied for $m = 2$, $n \geqslant 2$. Substitution of the expansions into equations (32), (33), (36) and (38), with condition (1) leads to the following expressions

$$\mu_1 = 2\pi(\lambda - 1), \tag{45}$$

$$\gamma_n = 2\pi n(\lambda - 1)\Theta_{n-1}, \tag{46}$$

$$F_n = -(\lambda - 1)n!\,\epsilon/2, \tag{47}$$

and

$$\Theta_{n-1} = \frac{(\lambda-1)^2}{4} n!\,\epsilon, \tag{48}$$

which, when used in equations (40), (41), (42) and (43), gives the values of these variables for small θ. For the case of $n = 2$, we use condition (3) which results in a cubic equation for Θ_1,

$$6\lambda^2\Theta_1^3 + (5\lambda^2 + 2\lambda)\Theta_1^2 + 2\Theta_1\left[\lambda - \frac{q_2(\lambda-1)^2}{2\lambda^2}\right] - \frac{q_2(\lambda-1)^2}{2\lambda^2} = 0, \tag{49}$$

as well as relations from which the other variables can be derived given the value of Θ_1. The equation has only one positive root and thus provides a unique value for Θ_1 and a unique way of starting the numerical solution.

3.2 NEAR THE EQUATOR

A similar analysis can be made near the equator, $\theta = \pi/2 - \eta \sim \pi/2$. In this case the expansion of q leads to the approximation

$$q(\eta) = (1 + \epsilon) - \tfrac{1}{2}\epsilon n\eta^2 = q_* + \tfrac{1}{2}q''_*\eta^2. \tag{50}$$

If we assume that the shell is smooth at the equator, $F'(\pi/2) = 0$, and that no mass accumulates there, $\Theta(\pi/2) = 0$, we can expand the variables in terms of η and so derive the following approximations

$$\mu(\eta) = \mu_* + \tfrac{1}{2}\mu''_*\eta^2, \tag{51}$$

$$F(\eta) = F_* + \tfrac{1}{2}F''_*\eta^2, \tag{52}$$

$$\Theta(\eta) = -\Theta'_*\eta, \tag{53}$$

$$\gamma(\eta) = -\gamma'_*\eta. \tag{54}$$

Using these approximations in equations (32), (33), (36) and (38) we derive a relation for λF_*

$$\lambda F_* = \frac{\lambda\sqrt{q_*}}{\lambda(\sqrt{q_*} - 1) + 1}, \tag{55}$$

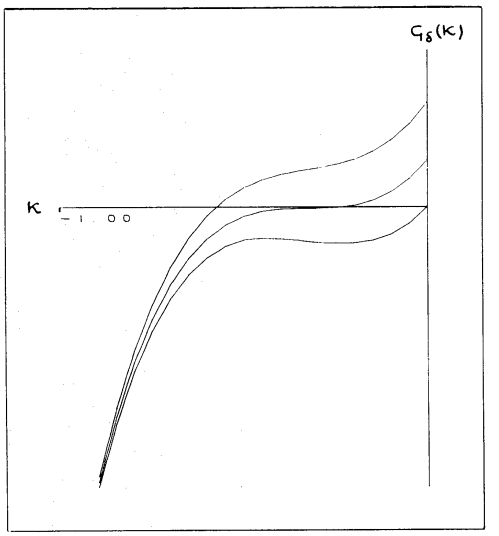

Figure 1. Plot of $G_\delta(\kappa)$ against κ for $\lambda F_* = 1.170$ and $\delta = 0.0$, 0.28 and 0.6.

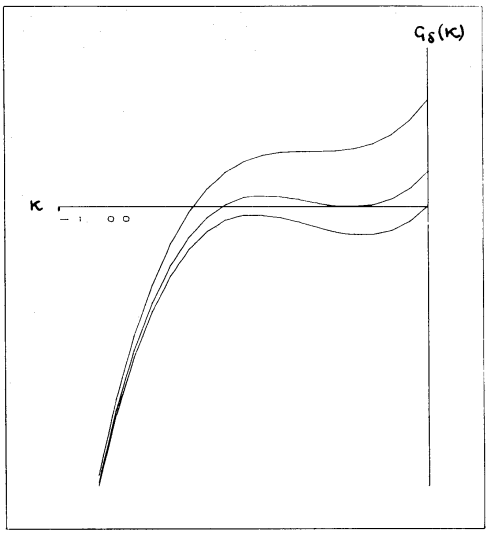

Figure 2. Same as Fig. 1 for $\lambda F_* = 1.406$, and $\delta = 0.0$, 0.25 and 0.77.

and a cubic equation for Θ'_*

$$G_\delta(\kappa) = 6X^2\kappa^3 + (5X^2 + X)\kappa^2 + (2X + \delta)\kappa + \delta = 0, \tag{56}$$

where $\kappa \equiv \Theta'_*$, $X \equiv \lambda F_*$ and $\delta \equiv -(q''_*/2q_*)(X-1)^2$. For a fixed value of X and variable δ, $G_\delta(\kappa)$ defines a set of curves of one of two different kinds. Those of the first kind (see Fig. 1) give a physical solution to equation (56) for all values of δ. For the second kind, Fig. 2, there is a critical value of δ, δ_c, above which the physical solution ceases to exist. A set of curves belongs to the first kind if the curve which has zero slope at the inflection point, $\kappa_{\rm inf}$, also has a negative or zero value at that point, $G_\delta(\kappa_{\rm inf}) \leqslant 0$. The inflection point is defined by

$$\frac{d^2}{d\kappa^2} G_\delta(\kappa) = 0, \tag{57}$$

and is $\kappa_{\rm inf} = -(5X+1)/18X$, which is independent of δ. Consider the curve which has zero slope at this point, so that $dG_\delta(\kappa_{\rm inf})/d\kappa = 0$; it defines a unique value

$$\delta = (25X - 1)(X - 1)/18, \tag{58}$$

and we find that $G_\delta(\kappa_{\rm inf}) \leqslant 0$ for this curve, if $X \equiv \lambda F_* \leqslant 1.181$. For $\lambda F_* > 1.181$, each family of curves has one curve with a double root which has a positive second derivative [$G_\delta(\kappa) = dG_\delta(\kappa)/d\kappa = 0$, $d^2G_\delta(\kappa)/d\kappa^2 > 0$]. This curve defines the value of δ_c for the family. From the first equality we derive a relation between λF_* and κ:

$$\lambda F_* = \frac{-(\kappa^2 + 2\kappa + 2)}{(12\kappa^3 + 23\kappa^2 + 10\kappa)}. \tag{59}$$

This can then be used to define δ_c in terms of κ,

$$\delta_c = \frac{2(3\kappa^2 + 12\kappa + 5)(\kappa^2 + 2\kappa + 2)}{(12\kappa^2 + 23\kappa + 10)^2}. \tag{60}$$

Table 1. Values of λF_* and δ_c derived as a function of $\kappa = \Theta'_*$ from equations (59) and (60). $|q''_*/q_*|_c$ is derived from the definition of δ.

$-\kappa$	λF_*	δ_c	$\left\|\frac{q''_*}{q_*}\right\|$
0	∞	0.200	0
0.05	4.285	0.213	0.039
0.10	2.315	0.227	0.262
0.15	1.684	0.242	1.035
0.20	1.395	0.258	3.315
0.25	1.250	0.273	8.750
0.30	1.188	0.285	16.084
0.325	1.181	0.287	17.513

We now use a continuity argument to establish that cusps must occur at the equator in models for which $\lambda F_* > 1.181$ and $\delta > \delta_c$. Consider a sequence of cases in which the slow stellar wind has an angular distribution of mass flow given by $1 + \epsilon h(\theta)$, with $h''(\pi/2)$ negative. Now compare successive patterns as ϵ increases from zero. For $\epsilon = 0$ the slow wind has spherical symmetry, and the appropriate solution of equation (56) is $\kappa = 0$. Clearly there is no cusp. The value of δ is proportional to $-h''$, and increases with ϵ. We expect to find a small change in κ for a small change in ϵ or in δ. It can be seen from Figs 1 and 2, that the curve $G_\delta(\kappa)$ is raised when δ increases and that the appropriate root of κ moves to more negative values. For curves of the second kind we eventually reach a value of ϵ such that $\delta = \delta_c$; in other words the curve has a double root at a point where $G''_\delta(\kappa)$ is positive. Now let ϵ, and therefore δ, be increased further. The nearby roots for κ become complex, and so the family of smooth solutions terminates with the value of ϵ for which $\delta = \delta_c$. A larger ϵ must therefore imply the existence of a cusp at $\theta = \pi/2$. The cubic equation $G_\delta(\kappa) = 0$ can, of course, have other roots. However, our argument is that the only roots with physical significance are those which evolve smoothly from zero as ϵ increases from zero.

In Table 1 we list a few values of λF_*, δ_c and $|q''_*/q_*|_c = \frac{1}{2} n \epsilon (1 + \epsilon)$.

4 The results

In this section we present some results from our analysis in the form of a table and figures. We discuss the dependence of the resultant shape on the input parameters λ, ϵ and n, and finally, we discuss the areas in which the model can be developed.

In Table 2, we list the velocity of the shell at the equator, $UF(\pi/2)$, and the rate of injection of thermal energy into the shocked wind, L_w, for several values of λ, ϵ and n. In calculating these values, the mass-loss rate and velocity of the slow wind were set to $10^{-5} M_\odot$ per year and $10\,\mathrm{km\,s^{-1}}$ respectively. A higher value of λ therefore implies that the shell velocity is higher and so that L_w is greater. To determine the effect of λ on the shape, we fix ϵ and n and consider the conditions for the presence of cusps. The first condition derived above was that cusps may exist only if $\lambda F_* > 1.181$. This can be rewritten, using equation (55), as

$$\lambda > \frac{6.5}{6.5 - \sqrt{1+\epsilon}}, \tag{61}$$

Table 2. Values of shell velocity at the equator [$UF(\pi/2)$] and rate of injection of thermal energy into the shocked wind (L_W) for various values of λ, ϵ and n.

λ	ϵ	n	$UF(\pi/2)$ km s^{-1}	L_W ergs s^{-1}
2	1	2	15.5	$2.7\ 10^{32}$
3	1	2	19.0	$1.3\ 10^{33}$
4	1	2	22.6	$3.5\ 10^{33}$
5	1	2	26.4	$7.3\ 10^{33}$
3	5	3	13.7	$1.0\ 10^{33}$
3	5	4	13.8	$1.2\ 10^{33}$
3	5	5	13.9	$1.3\ 10^{33}$
3	3	2	15.0	$5.0\ 10^{32}$
3	6	2	13.4	$2.3\ 10^{32}$
3	18	2	11.805	$6.1\ 10^{31}$

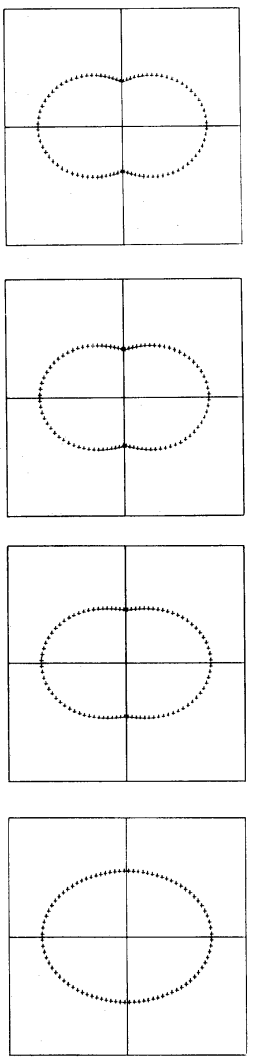

Figure 3. Shape of the nebula for $\epsilon = 1$, $n = 2$, and $\lambda = 2$ (bottom), 3, 4 and 5. It can be seen how the strength of the cusp increases with increasing λ. The axis of symmetry is horizontal.

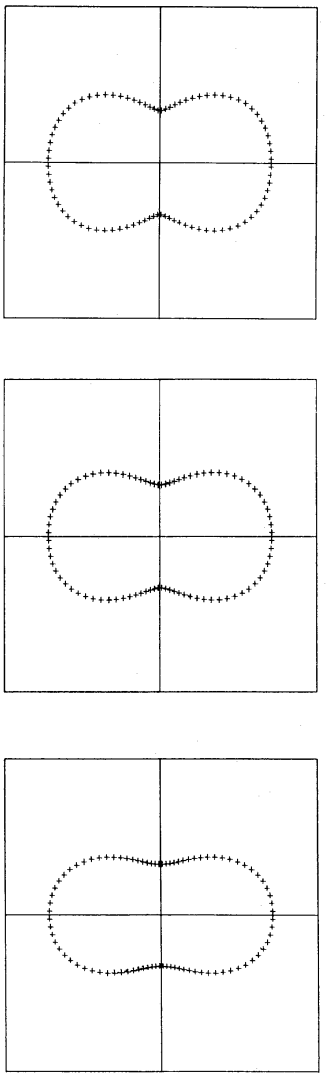

Figure 4. Shape of the nebula for $\lambda = 3$, $\epsilon = 5$, and $n = 3$ (bottom), 4 and 5. The strength of the cusps increases with n. We also note that the shape near the pole remains spherical to larger θ because the mass-loss rate of the slow wind is concentrated more and more towards the equator.

which is true for sufficiently large λ. However, for the existence of cusps, the second condition, $\delta > \delta_c$, must also be met. The expression for δ can be written in terms of λ, ϵ and n:

$$\delta = -\frac{n\epsilon}{4(1+\epsilon)}(\lambda F_* - 1)^2, \tag{62}$$

and so can be seen to increase with λ. Thus, as shown in Fig. 3, increasing λ will eventually lead to the presence of cusps for given ϵ and n.

The parameters ϵ and n determine the density distribution of the red-giant wind. As the velocity of the wind is taken to be constant, they relate only to the mass-loss rate (equation 1). The mass-loss rate at the equator exceeds that at the pole by a factor $1 + \epsilon$, which is linearly proportional to ϵ, but independent of n. Larger values of n mean that the mass-loss rate is more heavily weighted towards the equator, and a higher mass-loss rate is required at

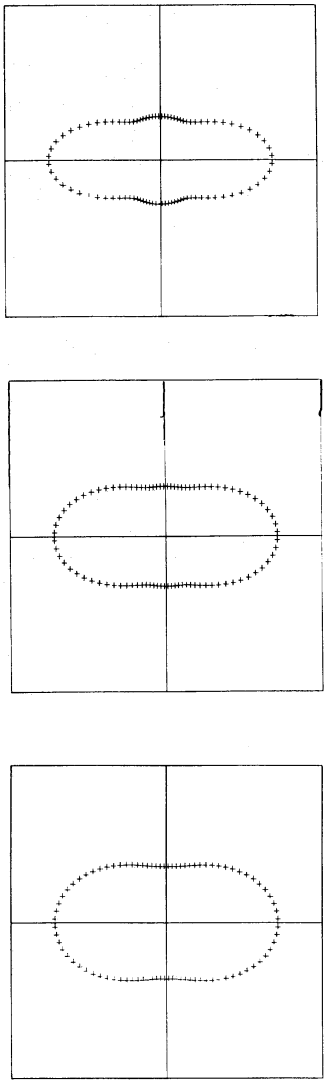

Figure 5. Shape of the nebula for $\lambda = 3$, $n = 2$, and $\epsilon = 3$ (bottom), 6 and 18. As ϵ increases, the cusp disappears and then is replaced by a bulge as $F'(\theta) \to 0$ for $\theta < \pi/2$.

the pole to compensate for the decrease at intermediate latitudes. As noted above, the first condition for cusps depends only on λ and ϵ. Rewriting relation (61) as

$$\epsilon < 42.3\left(\frac{\lambda - 1}{\lambda}\right)^2 - 1, \tag{63}$$

we see that, for given λ and n, cusps will only exist if ϵ is less than a certain value determined by λ. The second condition for cusps, the value of δ (equation 62), is not strongly dependent on ϵ. It is, however, linearly proportional to n. If the values of ϵ and λ are such that a cusp can exist, then as n increases so does the strength of the cusp (Fig. 4). Fig. 5 shows the effect of increasing ϵ. For ϵ sufficiently large, the value of $F'(\theta)$ approaches 0 and the radius becomes approximately constant at the equator so that a bulge appears, as shown in Fig. 5.

In conclusion, we note that there are several areas in which the model can be extended or improved. The strong shock approximation is expected to break down before the end of the

lifetime of the PN, and in some cases (Fig. 5, top) very early on. We have not dealt with the behaviour of the shell at the equator for the cases where oppositely directed flows meet (cusps), and we have neglected the finite temperature of the shell. The thickness of the shell is a function of θ, and is larger at the equator, so the ionization front will escape at the pole before the equator. For the same reason, the thin shell approximation will break down at the equator before the pole. These points will be dealt with in future work.

Acknowledgments

The authors thank John Dyson for useful discussions and Sam Falle for many helpful comments. KAW is supported by a research grant from the SERC.

References

Dyson, J. E. & de Vries, J., 1972. *Astr. Astrophys.*, **20**, 223.

Kahn, F. D., 1982. *Planetary Nebulae, IAU Symp. No. 103,* p. 305, ed. Flower, D. R., Reidel, Dordrecht, Holland.

Kwok, S., 1982. *Astrophys. J.*, **258**, 280.

Renzini, A., 1982. *Physical Processes in Red Giants*, p. 431, eds Iben, I. Jr. & Renzini, A., Reidel, Dordrecht, Holland.